Vol. 48, No. 1 (2026) 157-165, DOI: 10.24874/ti.2060.11.25.02

Tribology in Industry

www.tribology.rs

RESEARCH

A Study on the Adhesion Strength of WC Coatings on 1045 Steel Substrate Using HVOF

Tuan-Linh Nguyen[a], Hong Tien Nguyen[a,*]

[a]*School of Mechanical and Automotive Engineering, Hanoi University of Industry, Vietnam.*

Keywords:

HVOF
Coating
ANOVA
Adhesive strength
High-velocity oxy-fuel

* Corresponding author:

Hong Tien Nguyen
Email: nguyenhongtien@haui.edu.vn

Received: 4 November 2025
Revised: 6 December 2025
Accepted: 12 February 2026

A B S T R A C T

In the processing and manufacturing industries, many machine components operate under high-pressure, high-temperature, and high-friction conditions. Consequently, these components often wear out or fail quickly. To address this issue, surface treatment technologies are commonly employed to enhance the durability of machine parts. One such technology, which has been applied and proven effective, is the high-velocity oxy-fuel (HVOF) spraying method. This method can produce high-quality coatings on steel substrates. However, ensuring a strong bond between the coating and the steel substrate is a critical challenge, as harder coatings are more prone to delamination or peeling due to increased brittleness and the development of residual stresses during rapid particle acceleration and solidification in the HVOF process. This article presents the use of the Taguchi experimental method combined with ANOVA analysis to evaluate the adhesive strength of WC coatings on 1045 steel substrates when applied using the HVOF spraying method. The study aims to identify optimal spraying conditions to achieve the best adhesive strength, thereby improving the quality and lifespan of machine components by enhancing load transfer, wear resistance, and long-term service reliability.

1. INTRODUCTION

Adhesive strength is a crucial property of coatings, as it determines their performance, particularly in applications involving high-impact loads and significant friction [1]. When the coating lacks sufficient adhesive strength, these high-impact loads and friction forces can cause delamination, cracking, and eventual failure. Figure 1 illustrates examples of delamination (Fig. 1a) and cracking (Fig. 1b) in coatings.

The adhesive strength of coatings includes both the adhesion strength between the coating and the substrate and the bonding strength among the elements within the coating. Among these, the adhesion between the coating and the substrate is often emphasized, as the materials, states, and physical and chemical properties of the two are typically different, making it more challenging to achieve a strong bond. Coating bonds are primarily mechanical, determined by the impact level of the sprayed metal particles on the substrate.

Consequently, the temperature of the sprayed particles and the roughness of the substrate surface are two critical factors for achieving optimal coating adhesion.

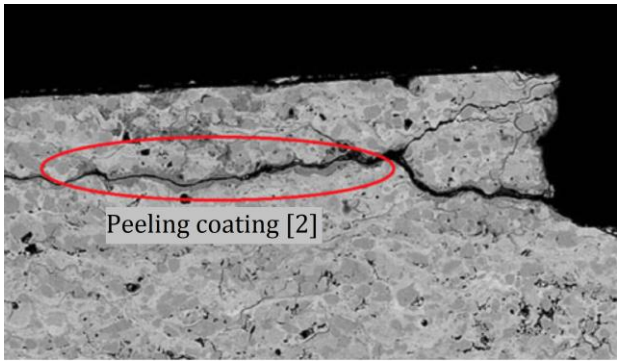

(a)

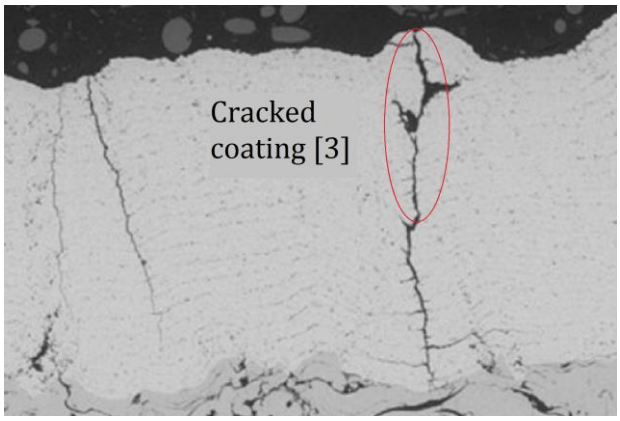

(b)

Fig. 1. Coating damage due to peeling [2] and cracking [3].

Delamination and cracking are commonly observed in hard and brittle coatings such as ceramic and WC-based cermet coatings when adhesion strength is insufficient or residual stresses are high [4].
WC-based coatings are widely used in high-load and severe wear applications due to their exceptional hardness, abrasion resistance, and thermal stability. When combined with metallic binders such as Ni, WC coatings offer a favorable balance between hardness and toughness, which is critical for components subjected to high mechanical stress. These characteristics make WC coatings a suitable material system for investigating adhesion behavior under HVOF spraying conditions.

When the kinetic energy of the metal particles is high, localized plastic deformation and partial melting occur upon impact, When the kinetic energy of the metal particles is high, localized plastic deformation and partial melting occur upon impact, leading to increased contact area, enhanced mechanical adhesion, and stronger interfacial bonding, as well as stronger atomic attraction between the two metal layers. For particles that do not melt or have already cooled upon reaching the surface, adhesion is achieved solely through mechanical forces. Research in [5] indicates that high particle velocities in the HVOF process facilitate melting-induced bonding, resulting in dense, low-porosity coatings with elevated adhesion strength. In research [4], the authors highlighted that the bonds within the coating consist of mechanical, metallic, and various chemical and physical interactions. Among these, mechanical bonds play the most critical role, locking the sprayed particles into the irregularities of the substrate and previously sprayed layers, thereby determining the adhesive strength of the coating.

Currently, various spraying methods are employed to enhance surface quality or restore damaged components. Among them, the High-Velocity Oxygen-Fuel (HVOF) method is notable for its numerous advantages [6]. The HVOF method generates very high particle velocities, typically in the range of several hundred to over 1000 m/s, depending on the spraying system and operating parameters. Such high particle velocities promote severe plastic deformation and effective splat formation upon impact, resulting in dense coatings with low porosity and improved adhesion strength. Compared with conventional thermal spray processes, the relatively lower flame temperature and higher kinetic energy of particles in HVOF spraying reduce particle overheating and oxidation, thereby enhancing interfacial bonding and coating integrity [4,7]. Compared to conventional plasma spraying, HVOF typically produces higher particle velocities, lower porosity coatings, and improved adhesion due to reduced particle overheating and oxidation. As a result, coatings produced by the HVOF method generally exhibit dense, well-consolidated microstructures with very low porosity [8]. These coatings also exhibit greater adhesive strength than those produced by conventional spraying methods [9]. However, achieving high adhesive strength in HVOF coatings depends critically on selecting appropriate spraying parameters. Research in this field has yielded significant results in enhancing coating durability.

For example, in the study [7], Christophe Lyphout and collaborators established relationships between process parameters, particle characteristics in flight, coating microstructure, and the adhesive strength of IN718 coatings using the HVOF method. In the study [10], the authors demonstrated that spraying parameters influence the porosity and hardness of coatings, thereby affecting their adhesive strength. Study [11] further emphasized the importance of these parameters. These studies are particularly significant for improving the durability and service life of machine components, especially those with complex shapes that are subject to multiple factors such as high temperature, high pressure, and intense friction. Examples include screws used in plastic extrusion machines, feed pellet mills, biomass pelletizers, and sawdust compaction machines.

Additionally, some studies, such as [12,13], have shown that optimized design solutions for component geometry before HVOF spraying can significantly improve the quality and service life of machine components. Therefore, combining design solutions with HVOF spraying techniques to enhance product performance is of considerable importance.

Although WC-based coatings deposited by the HVOF spraying process have been extensively investigated, most previous studies have primarily focused on wear resistance, hardness, and microstructural characteristics. In contrast, systematic investigations on adhesion strength - particularly those considering the combined effects and relative influence of key HVOF spraying parameters - remain limited for WC coatings applied on 1045 steel substrates. In addition, interaction effects among spraying parameters are often overlooked. Given that 1045 steel is widely used in load-bearing mechanical components, it represents a relevant and representative substrate for industrial applications. Therefore, this study aims to address this research gap by quantitatively evaluating the influence and interaction of spray flow rate, spray distance, and oxygen/propane ratio on adhesion strength using a combined Taguchi–ANOVA approach, thereby providing practical guidance for parameter optimization in industrial applications.

2. MATERIALS AND METHODS

2.1 The specimen

The specimen was fabricated using 1045 steel, which is commonly utilized in mechanical structures. Table 1 illustrates the chemical composition of 1045 steel [14].

The injection process was controlled using an HVOF spray device [10] (HP-2700 M), as shown in Figure 2.

Fig. 2. HVOF spray equipment.

Table 1. The chemical composition of 1045 steel.

Steel grade	C (%)	Si (%)	Mn (%)	P (%) max	S (%) max	Cr (%)
1045	0.42÷0.50	0.15÷0.35	0.50÷0.80	0.025	0.025	0.20÷0.40

Table 2. The chemical composition of the WC HMSP1060-00+60% 4070 spraying powder [14].

Chemical composition	C (%)	Ni (%)	Fe (%)	Cr (%)	Si (%)	B (%)	WC (%)
Ratio	2.96	27.59	1.85	6.45	2	1.4	57.75

Table 3. The physical properties of WC and Ni [15].

No	Properties	WC	Ni
1	Melting temperature (°C)	2785 ÷ 2830	1455
2	Young's modulus (GPa)	530 ÷ 700	200
3	Density (g/cm^3)	15.6	8.9

The chemical composition values reported in Table 1 correspond to the measured composition of the specific 1045 steel batch used in this study.

Main parameters of the HVOF injection equipment system: Spray flow (F = 15÷50 g/min), spray distance (D = 0.15÷0.5 m), oxygen/propane ratio (R = 2÷7), powder feeding accuracy (0.1 g/rev), the required control pressure from 0 to 11 bar, adjustable pressure within ±0.1 bar.

The specimen was coated with a layer of WC HMSP1060-00+60% 4070 powder, containing Nickel elements combined with Tungsten Carbide, which is known for its excellent friction and abrasion resistance. Its chemical composition is shown in Table 2.

The physical properties of WC and Ni are presented in Table 3.

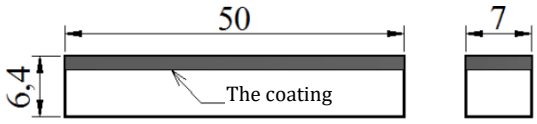

Fig. 3. The specimen.

After coating, the specimens were polished on both end faces to ensure a uniform compression cross-section. The WC coating was applied on the specimen, which was subsequently subjected to adhesion testing. The shape and dimensions of the specimen are shown in Figure 3.

2.2 Method of measuring adhesion strength

The adhesion strength of the coating to the substrate is tested using an experimental method. The adhesion strength test in this study was conducted in accordance with the Vietnamese national standard TCVN 9349:2012, which is technically equivalent to the international standard ISO 4624:2002. In the present study, the test configuration applies a shear-dominated loading condition at the coating–substrate interface. Although TCVN 9349:2012 (ISO 4624:2002) primarily describes pull-off adhesion testing, the standard is referenced here for specimen preparation and general testing principles, while the stress calculation is adapted to the shear loading configuration used. After coating, the specimen (4) is placed in a mold (2) and clamped tightly by two bolts (3), as shown in Figure 4. A universal testing machine is used to apply compressive force. This force causes the punch (1) to move downward vertically, generating shear stress (τ) and breaking the bond between the coating and the substrate.

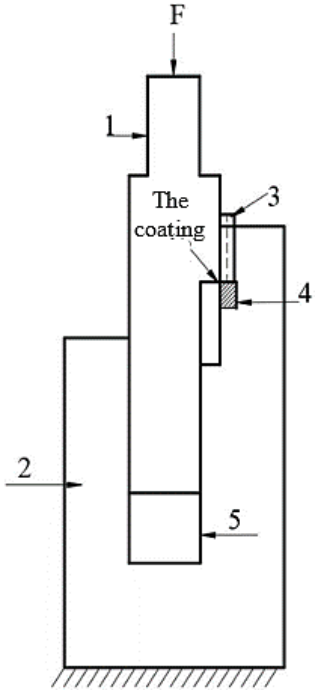

Fig. 4. Adhesion strength measurement diagram.

The compressive force is applied on the universal testing machine using a force-increasing method to determine the failure load of the bond layer. The shear stress, representing the adhesion strength, is calculated using (1).

$$\tau = \frac{F}{S} \tag{1}$$

where F is the bond breaking force (N), and S is the surface area of the bonding layer (mm^2), Here, S represents the effective cross-sectional area of the coating subjected to shear loading at the point of interfacial failure. In this study, the adhesion strength is defined as the maximum stress required to cause failure at the coating–substrate interface under the applied loading condition. The bonded area S corresponds to the effective cross-sectional area of the coating subjected to shear loading during the test.

The Taguchi experimental design method is used with three input parameters: flow rate of spray (F), spray distance (D), and oxygen/propane ratio (R). The Taguchi L9 orthogonal array [14,15], along with the measured results (τ) representing the adhesion strength of the coating, is shown in Table 4.

Table 4. Taguchi L9 table with measured τ values.

No	F (g/min)	D (m)	R	τ (MPa) (1st)	τ (MPa) (2nd)	τ (MPa) (3rd)	$\bar{\tau}$ (MPa)
1	25	0.2	4	52.4	50.7	52.0	51.7
2	25	0.25	5	57.9	60.2	58.2	58.8
3	25	0.3	6	62.7	63.1	62.5	62.8
4	30	0.2	5	56.5	55.8	55.2	55.8
5	30	0.25	6	63.1	65.5	64.6	64.4
6	30	0.3	4	58.3	57.9	59.5	58.6
7	35	0.2	6	58.5	59.0	57.9	58.5
8	35	0.25	4	56.6	57.2	58.5	57.4
9	35	0.3	5	65.8	64.2	66.1	65.4

To analyze the influence of F, D, and R on the adhesion strength of the coating, utilize the SN_i factor [14]:

$$SN_i = -10\,log(\sum_{u=1}^{N_i} \frac{y_u^2}{N_i}) \quad (2)$$

where i = 1÷9, u is number of experiments (u = 1÷3), N_i is number of tests for experiment i (N_i = 3), so SN_i coefficient is calculated as shown in Table 5.

Table 5. The SN_i coefficient is calculated for τ.

No	F (g/min)	D (m)	R	τ (N/mm²)
				SN_i
1	25	0.2	4	-34.2707
2	25	0.25	5	-35.3839
3	25	0.3	6	-35.9546
4	30	0.2	5	-34.9383
5	30	0.25	6	-36.1787
6	30	0.3	4	-35.3536
7	35	0.2	6	-35.3384
8	35	0.25	4	-35.1841
9	35	0.3	5	-36.3078

The SN coefficient is calculated for each level as follows:

$$SN_{P1,1} = \frac{(SN_1 + SN_2 + SN_3)}{3};$$

$$SN_{P1,2} = \frac{(SN_4+SN_5+SN_6)}{3}; SN_{P1,3} = \frac{(SN_7+SN_8+SN_9)}{3}$$

$$SN_{P2,1} = \frac{(SN_1+SN_4+SN_7)}{3}; SN_{P2,2} = \frac{(SN_2+SN_5+SN_8)}{3}$$

$$SN_{P2,3} = \frac{(SN_3+SN_6+SN_9)}{3}; SN_{P3,1} = \frac{(SN_1+SN_6+SN_8)}{3}$$

$$SN_{P3,2} = \frac{(SN_2+SN_4+SN_9)}{3}; SN_{P3,3} = \frac{(SN_3+SN_5+SN_7)}{3}$$

The SN values for each level are shown in Table 6.

Table 6. The SN factor for each level affecting coating adhesion strength.

Level	τ		
	SN calculated for F	SN calculated for D	SN calculated for R
1	-35.2031	-34.8491	-34.9361
2	-35.4902	-35.5823	-35.5433
3	-35.6101	-35.872	-35.8239
Delta	0.407	0.2898	0.8878
Rank	2	3	1

The oxygen/propane ratio exhibits the highest Delta value and ANOVA contribution, confirming its dominant influence on adhesion strength.

In the context of this study, the values of delta and rank are used to evaluate the relative influence of each process parameter on the adhesion strength of the WC coating. The delta value represents the difference between the maximum and minimum average adhesion strength observed across the levels of a given factor. Therefore, the larger the delta, the more significant the effect of that parameter on the response. This ranking allows to identify which process parameters have the most substantial effect and should be prioritized in optimization.

3. RESULTS AND DISCUSSION

ANOVA analysis is used to evaluate the effect of each main parameter (F, D, R) and the interaction effects between these parameters on the adhesion strength of the coating. The results are shown in Figure 5 and Figure 6.

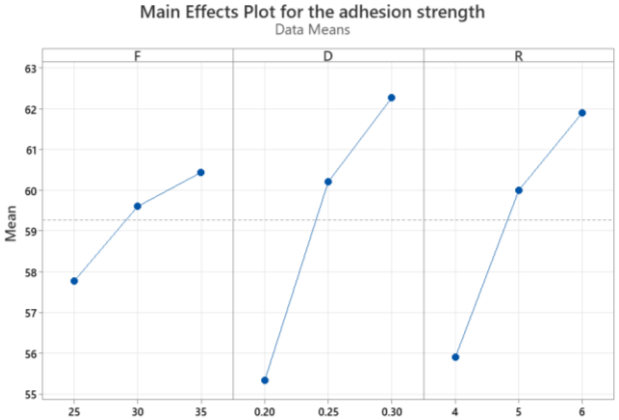

Fig. 5. The graph shows the influence of each main parameter on the adhesion strength of the coating.

From Figure 5, it is evident that within the examined range, the adhesion strength of the coating shows a clear relationship with the spray flow rate, spray distance, and oxygen/propane ratio. As the spray flow rate increases, the adhesion strength of the coating also increases, reaching its highest point at a flow rate of F = 35 g/min. As shown in Table 6, this suggests that a higher flow rate provides more material for the coating process, leading to a stronger bond between the coating and the substrate. This may be attributed to the increased amount of particles being deposited, which enhances the mechanical interlocking and overall adhesion. Similarly, as the spray distance increases, the adhesion strength improves, with the best result observed at D = 0.3 m. This could be because, at a certain distance, the particles have a higher velocity when they impact the substrate, resulting in better bonding. The optimal distance of 0.3 meters indicates a balanced approach where the particles still retain sufficient energy to create a strong bond but are not too far from the surface to lose their effectiveness upon impact. Furthermore, as the oxygen/propane ratio increases, the adhesion strength of the coating also improves, with the optimal ratio at R = 6. The oxygen/propane ratio influences the combustion temperature and the energy of the spray particles. A higher oxygen content typically leads to higher combustion temperatures, which in turn improves the quality of the coating by enhancing the fusion of particles and their adhesion to the substrate. The optimal ratio of R = 6 suggests a finely tuned balance where the combustion is efficient enough to provide sufficient heat for optimal particle bonding, without excessive oxidation or incomplete combustion.

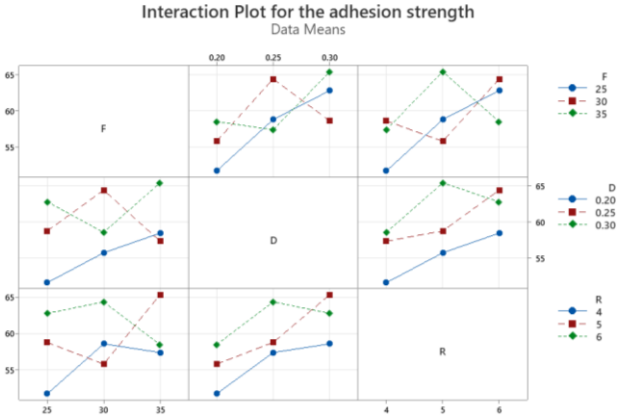

Fig. 6. The graph shows the interaction effects of the parameters on the adhesion strength of the coating.

From Figure 6, it can be observed that the spray parameters and the oxygen/propane ratio have different effects on the outcome of the process. The strong interaction between the spray flow rate and spray distance indicates that a change in one factor can directly affect the effectiveness of the other factor, while the weak interaction between the spray flow rate and the oxygen/propane ratio suggests that the oxygen/propane ratio plays a more important role in controlling the process. Finally, the almost negligible interaction between the spray distance and the oxygen/propane ratio shows that these two factors do not directly influence each other, with the oxygen/propane ratio being the key determining factor in the HVOF spraying process.

The experimental results also allow us to develop a regression mathematical equation representing the relationship between the adhesion strength of the coating and the spray parameters. This relationship is expressed by equation (3).

$$\tau = 13.97 - 0.3667F + 121.7D + 5.8R - 0.02F^2 - 553.3D^2 - 0.1667R^2 + 7.467F * D - 0.0067F * R \quad (3)$$

Table 7. Comparison between predicted and experimental optimum adhesion strength.

Parameter setting (F, D, R)	Predicted (MPa)	Experimental (MPa)	Difference (%)
35 g/min, 0.3 m, 6	67.9	65.4	3.8

The comparison presented in Table 7 confirms that the predicted optimum adhesion strength obtained from Equation (3) is in good agreement with the experimental value measured under the optimal spraying parameters. The percentage difference of approximately 3.8% demonstrates the reliability of the regression model within the investigated parameter range.

From mathematical equation (3), we can construct graphs that illustrate the relationship between adhesion strength and each pair of parameters: spray flow rate and spray distance (Fig. 7a), spray distance and oxygen/propane ratio (Fig. 7b), and oxygen/propane ratio and spray flow rate (Fig. 7c), as shown in Figure 7.

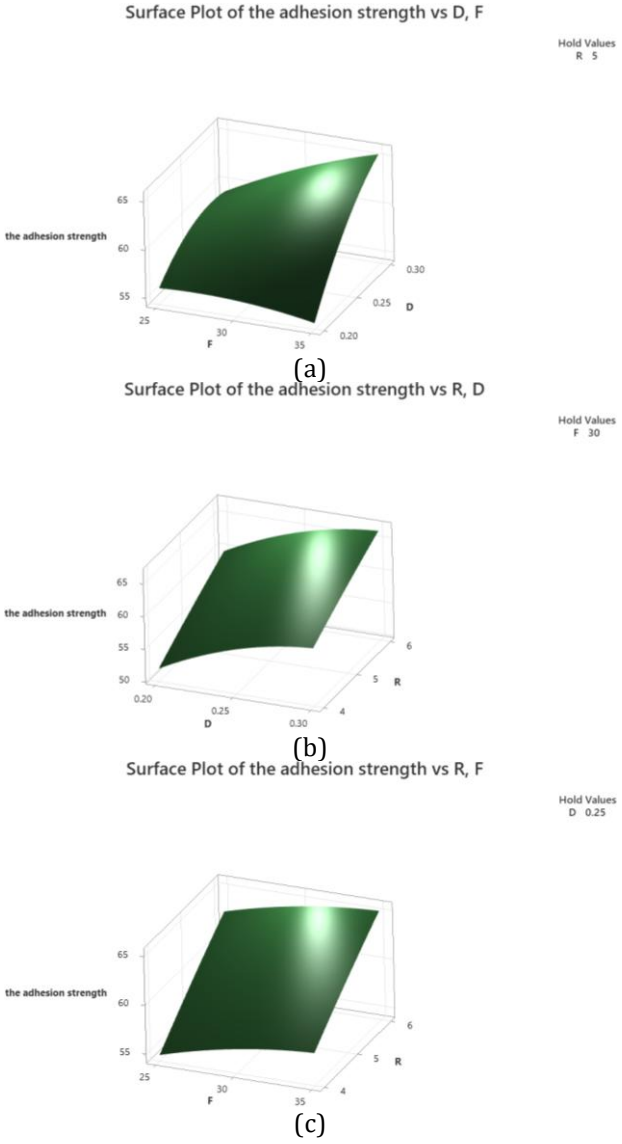

Fig. 7. The graphs show the relationship between adhesion strength and each pair of input parameters.

The analysis results clearly indicate that the oxygen/propane ratio plays the most dominant role in determining the adhesion strength of the coating. ANOVA analysis was performed using Minitab 19 (licensed version). This conclusion is further supported by the ANOVA results, which show that the oxygen/propane ratio has the highest contribution and statistical significance among the investigated parameters [16,17]. This parameter directly affects the combustion temperature, particle velocity, and thermal energy transfer during the spraying process. A well-optimized oxygen/propane ratio ensures proper combustion, enhancing particle fusion and interfacial bonding between the coating and the substrate. In contrast, deviations from the optimal ratio can lead to incomplete combustion, oxidation, or reduced particle velocity, all of which can significantly reduce adhesion strength.

Following the oxygen/propane ratio, the spray flow rate emerges as the second most influential parameter. An increase in the spray flow rate generally improves adhesion strength by increasing the amount of coating material available for deposition. However, excessive spray flow rates may result in particle crowding, inconsistent heating, or poor particle acceleration, ultimately reducing the coating quality. Therefore, maintaining an optimal flow rate, as observed at F = 35 g/min, is essential for achieving high adhesion strength.

Among the three parameters, the spray distance has the least significant influence on adhesion strength. While it still plays a role in determining particle velocity and impact energy, its effect is less pronounced compared to the oxygen/propane ratio and spray flow rate. The optimal distance, D = 0.3 m, provides a balance between particle heating and velocity, allowing the particles to reach the substrate with sufficient thermal and kinetic energy for effective bonding. However, variations in distance within the examined range exhibit less dramatic changes in adhesion strength compared to the other parameters.

The substantial difference in the degree of influence among these parameters highlights the need for careful optimization in HVOF spraying processes. Within the experimental range, the optimal combination of parameters F = 35 g/min, D = 0.3 m, and R = 6 yields the best adhesion strength results. The optimal condition of F = 35 g/min, D = 0.3 m, and R = 6 can be explained based on particle kinetic energy and bonding efficiency. A higher spray flow rate increases particle momentum, promoting plastic deformation and interlocking at the interface. A spray distance of 0.3 m ensures sufficient particle velocity while avoiding excessive cooling before impact. Meanwhile, an oxygen/propane ratio of 6 provides an optimal combustion balance, enhancing particle acceleration without causing excessive oxidation. The combined effect of these parameters results in improved adhesion strength. This combination represents an ideal balance, ensuring proper thermal energy, material deposition, and particle velocity for creating a high-quality coating. This result

confirms the reliability of the proposed regression model, while further studies involving additional spraying parameters are required.

The predicted optimum adhesion strength obtained from the regression model shows good agreement with the experimental result under the optimal HVOF spraying parameters. This close agreement confirms the validity of the Taguchi–ANOVA-based optimization approach and demonstrates its reliability for predicting adhesion performance of WC coatings on 1045 steel substrates.

4. CONCLUSIONS

Through a systematic experimental investigation supported by Taguchi design and ANOVA analysis, the influence and relative importance of HVOF spraying parameters on the adhesion strength of WC coatings on 1045 steel substrates were clarified. The results allow clear identification of dominant factors and optimal spraying conditions. The main conclusions of this study can be summarized as follows:

- The oxygen/propane ratio was identified as the most influential parameter affecting the adhesion strength of WC coatings on 1045 steel substrates. • Spray flow rate exhibited a secondary influence on adhesion strength, while spray distance showed the least effect within the investigated parameter range.
- The optimal HVOF spraying parameters for maximizing adhesion strength were determined as F = 35 g/min, D = 0.3 m, and R = 6.
- The Taguchi–ANOVA analysis and regression model provided consistent results, demonstrating the reliability of the proposed optimization approach.
- The findings offer practical guidance for improving coating adhesion and reliability in industrial applications involving WC coatings deposited by HVOF spraying.
- The present study is limited to three HVOF spraying parameters within a defined experimental range. Future work will focus on additional process parameters, microstructural characterization, and extended performance evaluation under more severe service conditions.

REFERENCES

[1] D. Vu, "Prediction of the Adhesion Strength of Coating in Plasma Spray Deposition," *Engineering, Technology & Applied Science Research*, vol. 13, no. 2, pp. 10367–10371, 2023, doi: 10.48084/etasr.5673.

[2] L. Vernhes, David A. Lee, D. Poirier, D. Li, and J. E. Klemberg-Sapieha, "HVOF Coating Case Study for Power Plant Process Control Ball Valve Application" *Journal of Thermal Spray Technology*, vol. 22, pp. 1184–1192, 2013, doi: 10.1007/s11666-013-9978-8.

[3] N. Curry, K. VanEvery, T. Snyder and N. Markocsan, "Thermal Conductivity Analysis and Lifetime Testing of Suspension Plasma-Sprayed Thermal Barrier Coatings", *Coatings* (MDPI), vol. 4, no. 3, pp. 630-650, 2014 doi: 10.3390/coatings4030630.

[4] C. J. Li, X. T. Luo, S. W. Yao, G. R. Li, C. X. Li, and G. J. Yang, "The bonding formation during thermal spraying of ceramic coatings: A review," *Journal of Thermal Spray Technology*, vol. 31, pp. 780–817, 2022, doi: 10.1007/s11666-022-01379-z.

[5] M. Abbas, G. M. Smith and P. R. Munroe, " Microstructural investigation of bonding and melting-induced adhesion in HVOF-sprayed coatings," *Surface and Coatings Technology*, vol. 402, No. 4, 2020, doi: 10.1016/j.surfcoat.2020.126353.

[6] G. Padmavathia, B. N. Sarada, S.P. Shanmuganatan, H. Ramesha, B.V. Padmini and R. Krishnamurthy, "A comparative assessment on the characteristics of HVOF sprayed cermet coatings," *Australian Journal of Mechanical Engineering*, vol. 22, no. 2, 2024, doi: 10.1080/14484846.2022.2100044.

[7] C. Lyphout, P. Nylen, and L. G. Östergren, "Adhesion strength of HVOF sprayed IN718 coatings," *Journal of Thermal Spray Technology*, vol. 21, pp. 86–95, 2012. doi: 10.1007/s11666-011-9689-y.

[8] W. Guaglianoni, M.A. Cunha, C.P. Bergmann, C. Fragassa, A. Pavlovic, "Synthesis, Characterization and Application by HVOF of a WCCoCr/NiCr Nanocomposite as Protective Coating Against Erosive Wear," *Tribology in Industry*, vol. 40, no. 3, pp. 477–487, 2018, doi: 10.24874/ti.2018.40.03.13.

[9] T. Widjajanto, D. B. Darmadi, Y. S. Irawan and F. Gapsari, "Comparative microstructure characteristics and properties of arc-sprayed Fe-based and HVOF-sprayed Ni-based coatings on ASME SA 210 C steel tube," *Results in Engineering*, vol. 17, no. 1, 2023, doi: 10.1016/j.rineng.2023.100985.

[10] T. L. Nguyen, H. T. Nguyen, V. T. Nguyen and D. D. Khuat, "Analysis of the effect of spray mode on coating porosity and hardness when spraying press screws by the high velocity oxy fuel method," *EUREKA: Physics and Engineering*, no. 6, pp. 93–103, 2023, doi: 10.21303/2461-4262.2023.003161.

[11] H. T. Nguyen, T. L. Nguyen, V. T. Nguyen and L. Hoang, "Investigation of the Impact of HVOF Spraying parameters on the Abrasion Resistance of Tungsten Carbide Coatings," *Engineering, Technology & Applied Science Research*, vol. 14, no. 6, pp. 17769–17773, 2024, doi: 10.48084/etasr.7996.

[12] H. T. Nguyen, T. L. Nguyen, V. T. Nguyen and V. Q. Phan, "Enhancement of Wear Resistance of High-Load Pressing Screw in Smokeless Charcoal Production by Using Genetic Algorithm and Discrete Element Method," *Tribology in Industry* , vol. 46, no. 1, pp. 151–162, 2024, doi: 10.24874/ti.1568.11.23.01.

[13] A. Muthulingam and E. Uhlmann, "Simulative investigation of the influence of different abrasive coating structures in double face grinding," *Journal of Machine Engineering*, vol. 24, no. 4, pp. 57–64, 2024, doi: 10.36897/jme/196196.

[14] J. E. Bringas, *Handbook of Comparative World Steel Standards*. West Conshohocken, PA, USA: ASTM International, 2004.

[15] J. R. Davis, *Handbook of Thermal Spray Technology*. Materials Park, OH, USA: ASM International, 2004.

[16] D. C. Montgomery, *Design and Analysis of Experiments*, 10th ed. Hoboken, NJ, USA: John Wiley & Sons, 2019.

[17] J. S. Arora, *Introduction to Optimum Design*, 3rd ed. Waltham, MA, USA: Elsevier, 2012.